Available online at www.sciencedirect.com
SCIENCE DIRECT®
Journal of Catalysis 219 (2003) 320–328
JOURNAL OF CATALYSIS
www.elsevier.com/locate/jcat

Adsorption of ethylene, benzene, and ethylbenzene over faujasite zeolites investigated by the ONIOM method

S. Kasuriya,[a] S. Namuangruk,[a] P. Treesukol,[a] M. Tirtowidjojo,[b] and J. Limtrakul [a,*]

[a] *Laboratory for Computational and Applied Chemistry, Kasetsart University, Bangkok 10900, Thailand*
[b] *The Dow Chemical Company, 2301 N. Brazosport Blvd, B-1226, Freeport, TX 77541-3257, USA*

Received 17 January 2003; revised 11 April 2003; accepted 29 April 2003

Abstract

The performance of the ONIOM (**O**ur-own-**N**-layered **I**ntegrated molecular **O**rbital + molecular **M**echanics) approach utilizing 10 combinations of two-layer ONIOM2 schemes has been tested for various sizes of faujasite clusters containing up to 84T tetrahedral atoms and the complexes they form with ethylene, benzene, and ethylbenzene molecules. Interaction energies of the adsorbates with a 3T bare quantum cluster are calculated to be −8.14, −7.48, and −7.76 kcal/mol at B3LYP/6-31G(d,p) level of theory, respectively. The long-range effects of the extended structure of zeolite were found to differentiate the stability of adsorption complexes that cannot be drawn from the typical 3T quantum cluster. The interaction energies of ethylene, benzene, and ethylbenzene molecules on the more realistic cluster, 84T, using ONIOM2(B3LYP/6-311++G(d,p):UFF) scheme are predicted to be −8.75, −15.17, and −21.08 kcal/mol, respectively, which compare well with the experimental estimates of −9.1, −15.3, and −19.6 kcal/mol, respectively. This finding clearly demonstrates that the interaction between adsorbate and acidic zeolites does not depend only on the Brønsted group center but also on the lattice framework surrounding the adsorption site. The results obtained in this study suggest that the ONIOM approach, when carefully calibrated, is a computationally efficient and accurate method for studying adsorption of aromatics on zeolites.

Keywords: Zeolite; Faujasite; ONIOM; QM/MM; Adsorption; Benzene; Ethylbenzene

1. Introduction

Ethylene, benzene, and their derivatives, including ethylbenzene and styrene, are among the most important chemicals in the chemical industry. Ethylbenzene is, commercially, the largest volume derivatives of benzene. Over 90% of the world's production of ethylbenzene is used in the manufacture of styrene, which is one of the most important industrial monomers. Other applications are paint solvents and pharmaceuticals [1]. The interaction between ethylene and benzene to ethylbenzene and the conversion of ethylbenzene to styrene are important industrial processes. The conventional processes of benzene alkylation are usually catalyzed by $AlCl_3$. This catalyst causes a number of problems concerning handling, safety, corrosion, and waste disposal [2]. An immense endeavor has been put into developing alternative catalyst systems that are more environmentally friendly. Nowadays the conventional $AlCl_3$-based processes have been progressively substituted with zeolite-based processes.

Zeolites are widely used in the petroleum and chemical industries as solid catalysts for a number of commercially important hydrocarbon reactions due to their outstanding properties, i.e., Brønsted and Lewis acid sites, size-shape selectivity, and thermal stability [3]. Using proton- and metal-zeolites as the catalysts can increase the percentage yield of the required products and thus reduce the production cost significantly. Zeolites have been used as effective catalysts in converting many hydrocarbon materials to value-added products. The adsorptions of ethylene, benzene, and ethylbenzene on zeolites, which are the elementary steps of the catalytic processes, have been studied experimentally by using FTIR [4–7] and NMR [8,9]. The adsorption energy of ethylene on the acidic H-Y zeolite was determined to be −9.1 kcal/mol [6]. The differential enthalpies of adsorption of benzene and benzene derivatives on H-Y zeolite were

* Corresponding author.
E-mail address: fscijrl@ku.ac.th (J. Limtrakul).

0021-9517/$ – see front matter
doi:10.1016/S0021-9517(03)00213-6

found to increase in the following order: benzene < ethylbenzene < 1,4-diethylbenzene ≈ 1,3-diethylbenzene [10].

Numerous theoretical models, including the periodic calculations, have been proposed to study the crystalline zeolite [11–19]. Nevertheless, zeolites that have a high impact in industrial processes usually possess hundreds of atoms per unit cell. This makes the use of sophisticated methods, such as periodic ab initio calculations, computationally too expensive and even impractical sometimes when very large zeolites are concerned. Therefore, the electronic properties of zeolites are usually modeled with quantum chemical methods for relatively small clusters where only the most important part of zeolites is focused [16–19]. With such limited models, the effect of the framework which can significantly change the structure and energetics of the system, is not taken into account. The recent development of hybrid methods, such as embedded cluster or combined quantum mechanics/molecular mechanics (QM/MM) methods [13,14, 20–25], as well as the more general ONIOM method has brought a larger system within reach of obtaining accurate results [26,27].

Up to date, the ONIOM method is applied to the study of extended systems, for example, chemical reactions on surface [28–33], and in enzymes [34]. However, there are no reports of the ONIOM method on H-FAU zeolites interacted with aromatic hydrocarbons.

In this study, we present the results of using the ONIOM model to represent the complicated structure of zeolites and to study the adsorption of ethylene, benzene, and ethylbenzene, which is the first important step for a more comprehensive study of alkylation reaction. Since the Brønsted acid site is considered as the active site for the alkylation of benzene [35–38] (although the adsorbates can be adsorbed at other sites), we limit the investigation to adsorption at the Brønsted acid site. We are focusing on the systems of faujasite (H-FAU), which are of high importance in many industrial reactions. The faujasite's unit cell of 576 atoms limits the use of periodic calculation, thus we use the ONIOM method to model the active site of H-FAU, the Brønsted acid site. The adsorption of ethylene, benzene, and ethylbenzene on the H-FAU has been investigated, and the rational choice of the levels of calculations for the ONIOM scheme has been examined. The results are compared to experimental data to find efficient combinations to satisfactorily reproduce the adsorption energies of H-FAU zeolites. This should provide us with a better understanding of the role of H-FAU in catalyzing the process of producing ethylbenzene.

2. Method

The cluster models were taken from the lattice structure of faujasite zeolite [39]. The 3T cluster $H_3SiOAl(OH)_2O(H)SiH_3$ (Fig. 1) is considered as the smallest unit required to represent the active site of zeolite. One of the silicon atoms in faujasite zeolites is substituted by an aluminum atom, and a proton is added to one of the oxygen atoms bonded directly to the aluminum atom. There are four distinct bridging configurations; the resulting structures will be called O1–H, according to the usual convention for the oxygen atoms in faujasite [39,40]. The Si–H bonds are fixed along the Si–O bonds of the faujasite framework [39]. The effect from the framework structure of zeolite cannot be totally neglected if more accurate results are required. Thus, the larger clusters were proposed for representing the system of protonated faujasite (H-FAU). The 20T model, illustrated in Fig. 2, is the 12-membered-ring window connecting two supercages of faujasite, including eight more tetrahedral atoms at the base next to the Al atom. The largest 84T cluster, including two supercages, acts as a nanoscopic reaction vessel (Fig. 3) where the adsorbates can be trapped inside.

Due to the limitation of computational resources and time consumption, the active region is treated more accurately with the ab initio method, while interaction in the rest of the model is approximated by a less accurate method.

According to the two-layer ONIOM approach, the calculation of energies can be simplified by treating the active region (i.e., the active Brønsted acidic site of a zeolite catalyst) with a high-level quantum mechanical (ab initio or density functional) approach, and the extended framework environment with a less expensive level, the HF, semiempirical, and molecular mechanics force fields methods. The total energy of the whole system can be expressed within the framework of the ONIOM methodology developed by Morokuma and co-workers,

$$E_{\mathrm{ONIOM2}} = E_{\mathrm{Low}}^{\mathrm{Real}} + \left(E_{\mathrm{High}}^{\mathrm{Cluster}} - E_{\mathrm{Low}}^{\mathrm{Cluster}}\right),$$

where the superscript Real means the whole system and the superscript Cluster means the active region, which would be treated with the higher level of calculation. Subscripts High and Low mean high- and low-level methodologies used in the ONIOM calculation. In this study, the high-level region is treated by the Hartree–Fock and the density functional theory with the hybrid functional B3LYP. The remainder is treated by molecular mechanics force fields (UFF) [41], semiempirical or the Hartree–Fock methods.

The accuracy of the QM/MM method, particularly the ONIOM method, depends significantly on the choice of the level of calculations for high- and low-level regions. Progressing through various types of quantum mechanics, semiempirical, and molecular mechanics methods, the experimental adsorption energy of the benzene/zeolite system can be used to validate the choice of methods. Using the B3LYP method for treating the quantum cluster, we varied the methods for the low-level region from the molecular mechanics force fields (UFF), semiempirical, over to the Hartree–Fock methods. Using the experimental observation as a benchmark, we found that the UFF method provides reasonable values corresponding to the experimental prediction. This is due to the explicit consideration of van der Waals contribution, which is the dominant contribution in adsorption-desorption in zeolites [42–47]. Therefore, the UFF method

is the practical choice for the low-level methodology when the high-level region is treated by the B3LYP/6-31G(d,p) method.

All calculations have been performed by using Gaussian98 code [48]. The basis set for the Hartree–Fock calculations is 3-21G, while the basis set 6-31G(d,p) is utilized for the B3LYP calculations. During the structure optimization, only the active site region, [≡SiO(H)Al(O)$_2$OSi≡], and the adsorbate are allowed to relax.

In order to obtain more reliable interaction energies, basis sets superposition error (BSSE) corrections were also taken into account. In addition, the common practice of running a higher level single-point energy calculation at the geometry generated by use of a cheaper method is as effective as performing all calculations at the higher level of theory. Thus, using the optimized geometries produced by the B3LYP/6-31G(d,p), we carried out the single-point energy calculations at the B3LYP/6-311++G(d,p) level.

3. Results and discussion

For the purpose of clarity, we separate the discussion below into two sections. In one section we compare the ONIOM results with experimental results. In the other section we focus mainly on the effects of the extended framework on the structural and energetic information of the interaction of ethylene, benzene, and ethylbenzene with H-FAU zeolites.

3.1. Comparison of ONIOM results with experimental results

Different two-layer ONIOM2 integrated schemes were performed on the ethylene, benzene, and ethylbenzene interaction with the different cluster models, as illustrated in Figs. 1–3. The faujasite zeolites were modeled by three different aluminosilicate clusters containing up to 84T tetrahedrally coordinated tetravalent atoms. Tables 1 and 2 list some

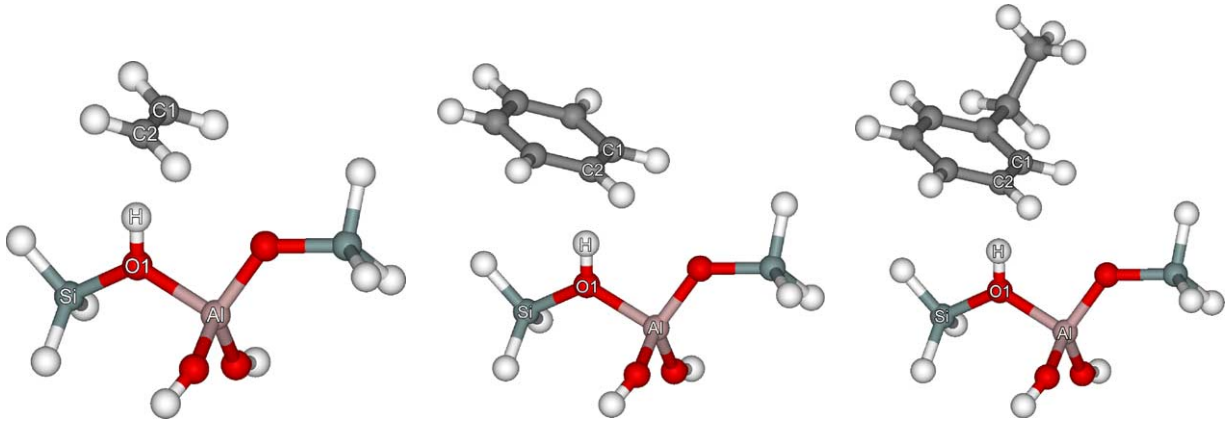

Fig. 1. Presentation of models of faujasite and interacting with adsorbates: (a) full 3T cluster model interacting with ethylene; (b) full 3T cluster model interacting with benzene; and (c) full 3T cluster model interacting with ethylbenzene.

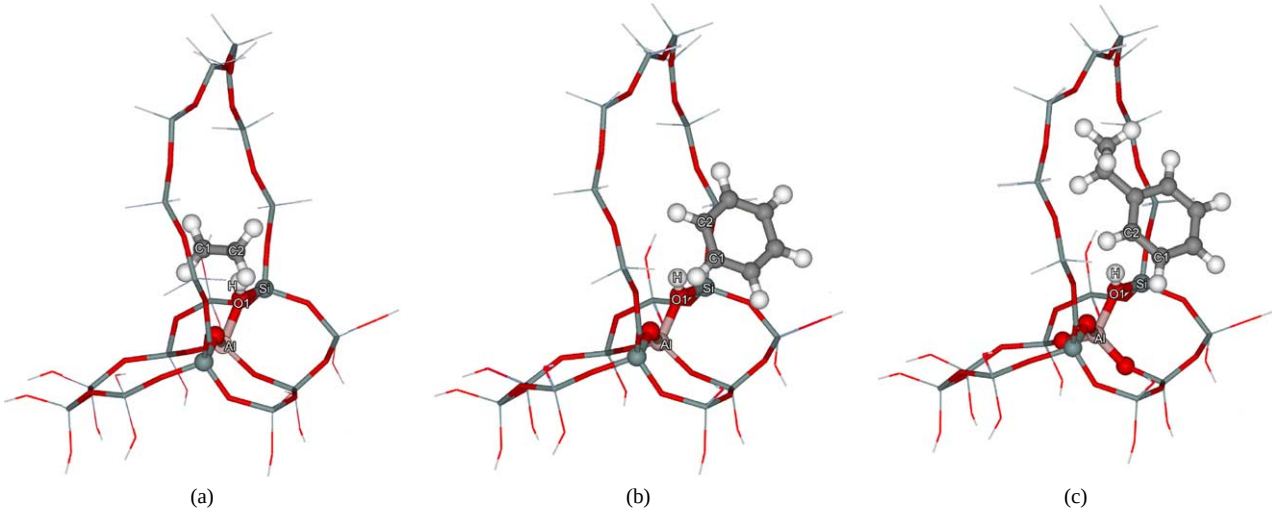

Fig. 2. Presentation of models of faujasite and interacting with adsorbates: (a) ONIOM2 layer models of 20T cluster interacting with ethylene; (b) ONIOM2 layer models of 20T cluster interacting with benzene; and (c) ONIOM2 layer models of 20T cluster interacting with ethylbenzene. Atoms belonging to the high-level regions are drawn as spheres.

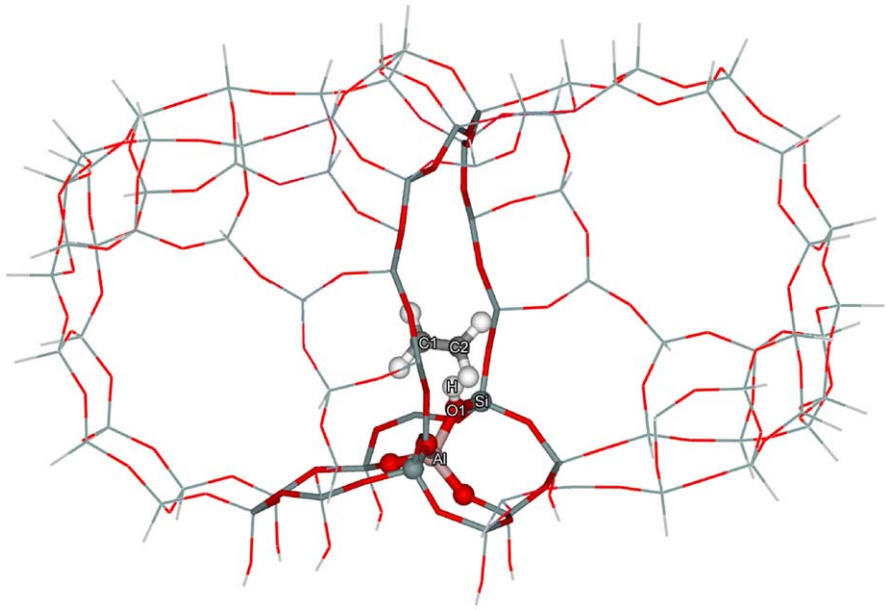

(a)

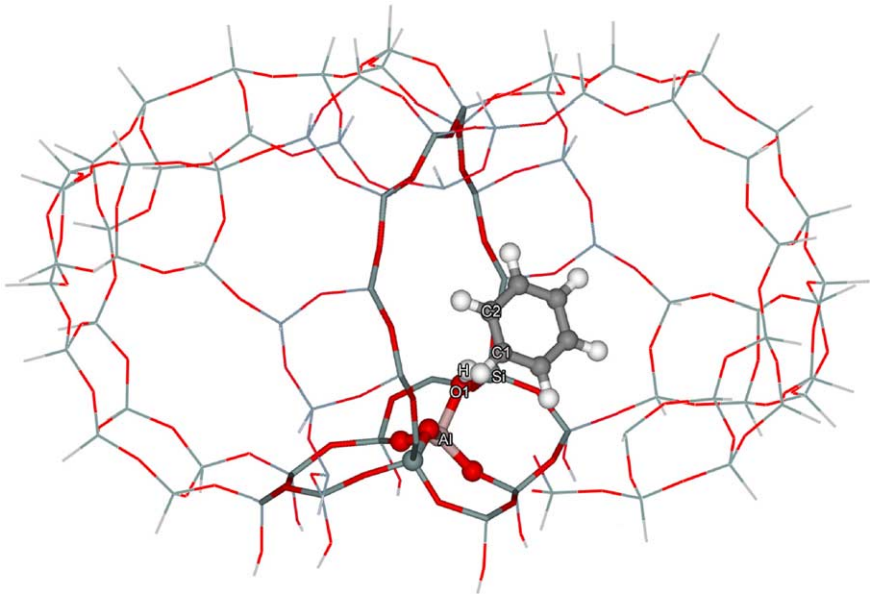

(b)

Fig. 3. Presentation of models of faujasite and interacting with adsorbates: (a) ONIOM2 layer models of 84T cluster interacting with ethylene; (b) ONIOM2 layer models of 84T cluster interacting with benzene; and (c) ONIOM2 layer models of 84T cluster interacting with ethylbenzene. Atoms belonging to the high-level regions are drawn as spheres.

selected structure parameters derived at 3T and 20T quantum clusters and the different two-layer ONIOM2 integrated schemes.

To assess the sensitivity of the active site structure with varying environments, we optimized the active site, [≡SiO(H)Al(O)$_2$OSi≡], for all the clusters, while the remaining atoms were kept fixed at the crystallographic positions. By comparing the structure between the full quantum cluster model of 3T and 20T models, it is seen that the cluster size environment has a little effect on the structure of the active site. The extended framework has the effect of lengthening the O1–H bond distance (Brønsted acid site) by 0.3 pm (full HF) and 0.2 pm (full B3LYP). In the ONIOM2 schemes, specifically B3LYP/6-31G(d,p):HF/3-21G and B3LYP/6-31(d,p):UFF, the O1–H bond distances are increased by 0.5 and 0.1 pm, respectively, thus enhancing the acidity of the Brønsted acid site.

Further support for the reliability of the active site subunit, [≡SiO(H)Al(O)$_2$OSi≡], by our calculations is given from NMR studies. Klinowski and co-workers have estimated the internuclear distance between the aluminum and the proton nuclei in a Brønsted acid site, r(Al···H),

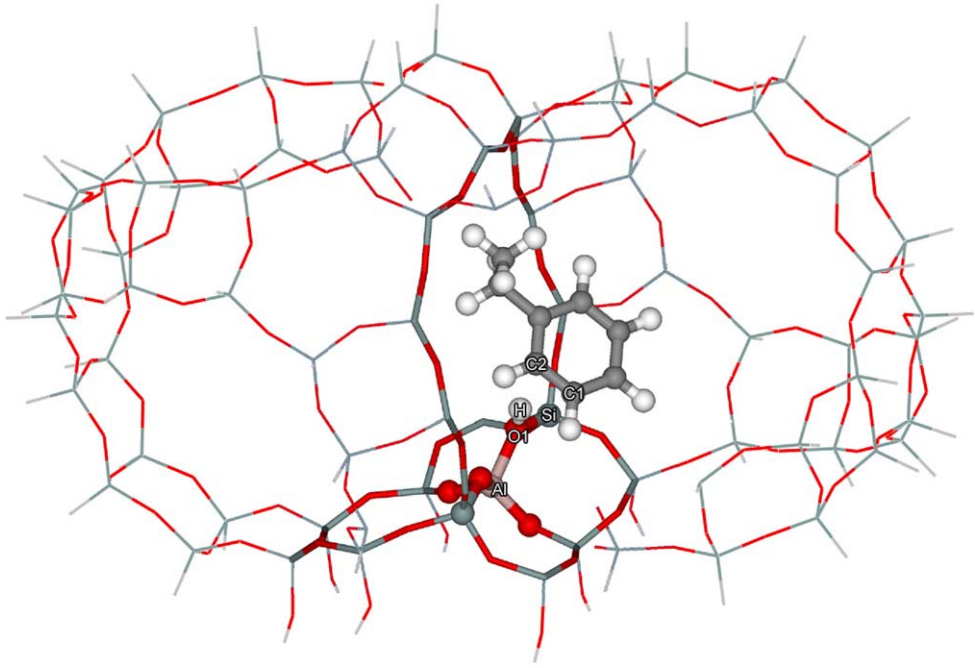

(c)

Fig. 3. Continued.

Table 1
Structural parameters of faujasite obtained at full HF/3-21G and various two-layer ONIOM2 schemes (bond distances in pm and bond angles in degrees)

Parameters	3T	20T					84T
	Full HF	Full HF	HF:MNDO	HF:AM1	HF:PM3	HF:UFF	HF:UFF
O1–H	96.8	97.2	96.9	97.0	96.8	96.8	96.8
Al–O1	184.2	185.6	183.0	183.2	185.8	180.5	180.5
Si–O1	171.9	170.1	171.3	167.5	172.1	169.4	169.4
∠Al–O1–Si	127.4	129.4	126.9	124.1	125.5	126.0	126.0
Al–H	233.5	239.6	231.5	230.3	235.6	230.2	230.3

The HF is Hatree–Fock with 3-21G basis set.

Table 2
Structural parameters of faujasite obtained at full B3LYP/6-31G(d,p) and various ONIOM2 schemes (bond distances in pm and bond angles in degrees)

Parameters	3T	20T						84T
	Full B3LYP	Full B3LYP	B3LYP:HF	B3LYP:MNDO	B3LYP:AM1	B3LYP:PM3	B3LYP:UFF	B3LYP:UFF
O1–H	96.7	96.9	97.2	96.8	96.8	96.7	96.8	96.8
Al–O1	191.6	191.4	193.7	190.1	191.1	193.8	186.0	186.0
Si–O1	170.9	170.4	168.2	170.5	166.0	170.8	168.6	168.6
∠Al–O1–Si	126.7	128.4	129.0	126.0	122.6	123.9	125.6	125.5
Al–H	246.0	250.8	254.3	243.4	244.6	249.6	240.0	240.2

The B3LYP is density functional theory with 6-31G(d,p) basis set; HF is Hartree–Fock with 3-21G basis set.

of faujasite [49] to be 238.0 ± 4 pm, whereas our computed r(Al···H) distance of 20T cluster is evaluated to be 240.0 pm at B3LYP/6-31G(d,p). It is noted that the computed r(Al···H) distances are underestimated in the cases of HF/3-21G combining with the semiempirical and molecular mechanics force fields [HF/3-21G:MNDO (231.5 pm), HF/3-21G:AM1 (230.3 pm), HF/3-21G:PM3 (235.6 pm), and HF/3-21G:UFF (230.2 pm)]. In comparison with the experimental data, the computed r(Al···H) distances using the ONIOM2 scheme are well represented generally by the B3LYP/6-31G(d,p), but not by the HF/3-21G which gives the r(Al···H) too small distances, specifically at the HF/3-21G:UFF (230.2 pm) vs B3LYP/6-31G(d,p):UFF (240.0 pm). The largest model of 84T at the B3LYP/6-31G(d,p):UFF shows structure parameters consistent with those of the 20T model. This suggests that B3LYP should be employed for a high-level model. Since the ONIOM2 (B3LYP:UFF) method gives a good structural representation of the Brønsted acid site and the UFF force field is also a theoretically appropriate method for representing the ef-

Table 3
Structure parameters for adsorbate/zeolite cluster complexes, where adsorbates are ethylene, benzene, and ethylbenzene

Methods	Parameters	3T			20T		
		Ethylene	Benzene	Ethylbenzene	Ethylene	Benzene	Ethylbenzene
HF	O1–H	97.7	97.5	97.6	98.9	98.1	98.4
	Al–O1	183.1	182.9	182.8	184.2	184.3	184.0
	Si–O1	171.0	171.1	171.0	169.1	169.5	169.4
	∠Al–O1–Si	127.5	127.7	127.7	129.5	129.3	127.6
	C1–H	226.3	220.6	217.2	219.4	244.0	220.8
	C2–H	226.5	224.8	225.8	227.4	252.0	250.6
	C=C	132.1	138.9	138.9	132.4	138.8	139.5
	qH	0.51	0.53	0.54	0.53	0.53	0.54
	qO1(H)	−1.01	−1.01	−1.01	−1.03	−1.02	−1.02
	qO2	−1.10	−1.10	−1.10	−1.12	−1.12	−1.12
B3LYP	O1–H	98.5	98.0	98.2	99.3	98.4	97.9
	Al–O1	189.9	189.8	189.7	189.1	189.6	189.9
	Si–O1	170.0	170.1	170.1	169.0	169.9	170.6
	∠Al–O1–Si	126.2	126.5	126.4	128.2	127.7	127.5
	C1–H	218.6	221.4	217.7	210.8	228.0	262.8
	C2–H	219.4	224.2	224.8	217.1	255.8	273.7
	C=C	133.7	140.1	140.0	133.8	140.2	140.5
	qH	0.36	0.38	0.38	0.37	0.38	0.38
	qO1(H)	−0.66	−0.66	−0.66	−0.67	−0.66	−0.66
	qO2	−0.71	−0.71	−0.71	−0.68	−0.68	−0.69

The zeolite clusters are 3T, 20T (bond distances in pm and bond angles in degrees). The B3LYP is density functional theory with 6-31G(d,p) basis set; HF is Hatree–Fock with 3-21G basis set.

fect of extended framework for this purpose (as discussed above) only the ONIOM models with the UFF force field will be discussed in detail hereafter.

3.2. Interactions of ethylene, benzene, and ethylbenzene with faujasite zeolites

Some structural parameters of the adsorption complexes calculated at finite clusters and at different ONIOM models (HF:UFF and B3LYP:UFF) are tabulated in Tables 3 and 4, respectively. Table 3 presents the comparison between the 3T and 20T cluster models of the adsorption complexes, indicating that adsorption does not significantly perturb structures of the adsorbed molecules or the zeolites due to the weak interactions between the hydrocarbons and the zeolite. Increasing cluster size has only a small effect on the structure of the active site, but significantly affects the orientation of the adsorbed molecules. For the small cluster models, the adsorbed molecules are Pi-bonded to the active site with almost equal bond distances between the two double-bond carbons and the Brønsted proton. For the 20T cluster models, interactions with the extended framework cause the adsorbed molecules to move farther from the acid proton and lose the symmetrical bidentated structures.

Table 4 shows structure parameters of the adsorption complexes calculated with the ONIOM2 method using 20T and 84T models showing that structures of the acid site are not affected by the increase of cluster sizes by enlarging the UFF outer layer. Similar to what was observed with the full quantum calculations at 20T, the adsorption does not significantly change the structures of the adsorbed molecules. Upon the adsorption of hydrocarbon on the acid site, the changes in Mulliken charges on acidic proton and bridging oxygen are minute. Increasing the quantum cluster size from 3T to 20T does not have any effect on the Mulliken charges on the acidic proton and its nearby oxygen atom (cf. Table 3). The same results are also observed for the ONIOM models (cf. Table 4). This suggests that the distribution of electron in the active region is not sensitive to the size of the cluster. However, significant changes in the orientation of the adsorbed molecules compared to the full quantum calculations of 20T models at B3LYP are observed. With the 84T ONIOM model at B3YLP:UFF, the adsorbed ethylene is moved slightly farther from the acid site and symmetrically bidentated to the Brønsted proton, while the adsorbed benzene and ethylbenzene are moved significantly closer to the zeolitic proton, possibly due to the confinement effect of the pore structure represented by the UFF force field.

The adsorption energy is one of the most valuable data obtained from experimental observation which can be used to validate the theoretical data. The adsorption energies of ethylene, benzene, and ethylbenzene on H-FAU zeolites calculated from different models, as discussed above, and also those from the ONIOM models using the semiempirical and molecular mechanics force fields for the outer layer are presented in Table 5.

Using the 3T cluster model, the DFT methods predict the adsorption energies of ethylene, benzene, and ethylbenzene to be −8.14, −7.48, and −7.76 kcal/mol, respectively. This is in contradiction with the experimental results. The adsorption energy of ethylene on the acidic H-FAU zeolite was determined to be −9.1 kcal/mol [6]. The adsorption energies of benzene and ethylbenzene on H-FAU ze-

Table 4
Structure parameters for adsorbate/zeolite cluster complexes, where adsorbates are ethylene, benzene, and ethylbenzene

Methods	Parameters	20T			84T		
		Ethylene	Benzene	Ethylbenzene	Ethylene	Benzene	Ethylbenzene
HF:UFF	O1–H	97.7	97.3	97.5	97.9	97.3	97.5
	Al–O1	179.7	179.7	179.4	179.6	179.4	179.4
	Si–O1	168.7	168.9	168.8	168.7	168.9	168.9
	∠Al–O1–Si	126.2	126.4	126.3	126.2	126.5	126.4
	C1–H	218.9	225.8	220.7	223.4	222.5	226.0
	C2–H	236.0	228.3	239.8	224.7	267.4	235.7
	C=C	132.2	139.0	138.8	132.2	138.7	138.9
	qH	0.52	0.53	0.54	0.52	0.53	0.54
	qO1(H)	−1.02	−1.01	−1.02	−1.03	−1.01	−1.02
	qO2	−1.11	−1.11	−1.11	−1.11	−1.11	−1.11
B3LYP:UFF	O1–H	98.9	98.2	98.3	98.9	98.0	98.1
	Al–O1	184.3	185.1	184.6	184.4	184.9	184.6
	Si–O1	167.5	168.2	168.1	167.6	168.4	168.1
	∠Al–O1–Si	125.3	124.9	125.0	125.3	124.9	125.2
	C1–H	214.6	217.3	215.4	214.5	219.1	229.7
	C2–H	214.7	239.7	236.1	215.2	259.4	231.0
	C=C	133.7	140.3	140.0	133.8	140.1	140.0
	qH	0.37	0.38	0.39	0.37	0.38	0.38
	qO1(H)	−0.64	−0.63	−0.63	−0.64	−0.63	−0.63
	qO2	−0.71	−0.69	−0.69	−0.71	−0.70	−0.70

The zeolite clusters are 20T, 84T (bond distances in pm and bond angles in degrees). The B3LYP is density functional theory with 6-31G(d,p) basis set; HF is Hatree–Fock with 3-21G basis set.

Table 5
Binding energy of ethylene, benzene, and ethylbenzene on the Brønsted proton of faujasite zeolites (binding energy in kcal/mol)

Methods/models	3T			20T			84T		
	Ethylene	Benzene	Ethylbenzene	Ethylene	Benzene	Ethylbenzene	Ethylene	Benzene	Ethylbenzene
B3LYP/6-31G(d,p)	−8.14	−7.48	−7.76	−10.93[a]	−14.28[a]	−15.90[a]	–	–	–
B3LYP/6-31G(d,p):UFF	–	–	–	−10.78	−14.94	−18.35	−11.49	−17.15	−22.99
B3LYP/6-31G(d,p)+BSSE[d]	−7.61	−6.54	−6.69	−10.25	−13.93	−17.30	−10.96	−16.15	−21.94
B3LYP/6-311++G(d,p)[b]	−5.39	−5.35	−5.78	−8.03	−12.23	−16.40	−8.75	−15.17	−21.08
HF/3-21G	−8.37	−9.49	−9.88	−10.90	−13.16	−17.23	–	–	–
HF/3-21G:UFF	–	–	–	−10.48	−16.76	−19.73	−11.43	−18.33	−24.09
HF/3-21G+BSSE[d]	−7.85	−8.42	−8.29	−10.05	−15.74	−18.50	−10.91	−17.21	−22.84
HF/6-311++G(d,p)[c]	−3.28	−3.47	−3.91	−6.21	−10.51	−11.74	−6.54	−13.69	−19.65
B3LYP/6-31G(d,p):HF/3-21G	–	–	–	−10.98	−11.40	−12.00	–	–	–
B3LYP/6-31G(d,p):MNDO	–	–	–	−6.99	−3.37	−3.23	–	–	–
B3LYP/6-31G(d,p):AM1	–	–	–	−7.67	−4.49	−4.99	–	–	–
B3LYP/6-31G(d,p):PM3	–	–	–	−5.41	−1.95	−1.13	–	–	–
HF/3-21G:MNDO	–	–	–	−7.10	−5.67	−5.65	–	–	–
HF/3-21G:AM1	–	–	–	−7.34	−6.50	−7.25	–	–	–
HF/3-21G:PM3	–	–	–	−5.63	−4.31	−4.12	–	–	–

Experimental adsorption energies of ethylene on H-FAU is −9.1 kcal/mol, taken from Ref. [6]. Experimental adsorption energies of benzene and ethylbenzene on H-FAU are −15.3l and −19.6 kcal/mol, respectively, taken from Ref. [10].

[a] Mixed basis sets of 6-31G(d,p) and 3-21G.

[b] Indicates single-point energy at indicated level of theory on the optimized B3LYP/6-31G(d,p): UFF structure.

[c] Indicates single-point energy at indicated level of theory on optimized HF/3-21G: UFF structure.

[d] Basis set superposition error corrected.

olites were experimentally measured to be -15.3 ± 1 and -19.6 ± 1 kcal/mol, respectively, indicating that the enthalpy of adsorption (ΔH_{ads}) of benzene is less than that of ethylbenzene [10].

Increasing the cluster size from 3T to 20T clusters, the calculated adsorption energies (ΔE_{ads}) of ethylene, benzene, and ethylbenzene interacted with zeolites are well differentiated (Table 5). Tests on the 20T clusters show that the ONIOM2 schemes, only the ONIOM2(B3LYP/6-31G(d,p):UFF) but not other ONIOM2 schemes, can be compared favorably with the full HF and B3LYP levels of theory. Using semiempirical methods, i.e., AM1, PM3, and MNDO for the outer layer, the wrong trend of ΔE_{ads} is observed as compared to the experimental data. The ONIOM2 model can substantially reduce the computational expense. For example, the single-point calculation

of the 20T/ethylene complex on an SGI machine (Origin 200) requires about 5 min (computational time) for the ONIOM2(B3LYP:UFF) method whereas, the full quantum cluster requires more than 50 min. This again confirms that the cost-effective ONIOM2 strategy should be utilized to obtain an accurate description of the system.

Increasing the cluster size from 20T up to the more realistic model, 84T, by enlarging the outer layer, the differences between each adsorption energy are pronounced. The adsorption energies of ethylene, benzene, and ethylbenzene calculated from the 84T cluster using ONIOM2 (B3LYP/6-31G(d,p):UFF) are calculated to be −11.49, −17.15, and −22.99 kcal/mol, respectively. These interaction energies are somewhat overestimated as compared to the experimental results. Including the basis set correction by single-point calculations at the higher basis set, 6-311++G(d,p), the corresponding interaction energies are predicted to be of −8.75, −15.17, and −21.08 kcal/mol. The BSSE corrections were also performed and gave similar results as the single-point calculations at the high basis set (see Table 5). These results are in good agreement with the experiment [6,10]. However, one may question if the energy could change if the model becomes bigger and bigger. To ensure the convergence of the ONIOM model, the structure optimization of a larger model of 336T with ethylbenzene has been carried out at the HF:UFF level of calculation. The adsorption energy of −24.60 kcal/mol from the 336T model is almost identical to the 24.09 kcal/mol from the 84T model at the same level of calculation, indicating that the use of the 84T ONIOM model is practical and increasing the model size would not have any profound effect on the energetics of the system.

It is noted that the choices of the methods using the high- and low-levels in the ONIOM scheme and also the sizes of the inner and outer regions are arbitrary. The size of the inner region employed in this study (3T cluster) is sufficient to represent the acid property of zeolites while small enough to guarantee that the van der Waals interactions between the hydrocarbon and the zeolite are well accounted for by the UFF force field, which is better than the DFT for this purpose [45–47]. Using the larger inner region, which may require the use of the MP2 level of theory in place of DFT, will be advantageous in searching for the transition state leading from ethylene and benzene to ethylbenzene. This challenging reaction is being actively pursued. From the structure and adsorption energy point of views, the B3LYP combining the UFF force fields method as a lower level is considered to be one of the best combinations for the ONIOM2 scheme. This efficient scheme provides a cost-effective computational strategy for treating the effects of a large extended framework structure.

4. Conclusions

The adsorption of ethylene, benzene, and ethylbenzene on H-FAU zeolites has been investigated with three different cluster sizes and methods comprising various two-level ONIOM2 schemes. The bare 3T B3LYP/6-31G(d,p) quantum cluster approach predicts the ethylene/H-FAU, benzene/H-FAU, and ethylbenzene/H-FAU complexes to have the binding energies of −8.14, −7.48, and −7.76 kcal/mol, respectively. The effect of the zeolite framework is modeled on the ONIOM2 method. We found that the extended framework significantly enhances their adsorption energy of adsorbates to the zeolites. In particular, the final predicted adsorption energies of −8.75, −15.17, and −21.08 kcal/mol, for the ethylene/H-FAU, benzene/H-FAU, and ethylbenzene/H-FAU complexes were calculated by the ONIOM2(B3LYP/6-311++G(d,p):UFF) scheme. This efficient scheme performs superbly when compared with the experimental estimates of −9.1, −15.3, and −19.6 kcal/mol, respectively. The results obtained in the present study suggest that the ONIOM approach yields a more accurate and practical model in studying the adsorption of unsaturated hydrocarbons on zeolites.

Acknowledgments

This work was supported in part by grants from the Thailand Research Fund (TRF Senior Research Scholar to J.L.) and the Kasetsart University Research and Development Institute (KURDI) as well as the Ministry of University Affairs under the Science and Technology Higher Education Development Project (MUA-ADB funds). The support from the Dow Chemical Company (USA) is also acknowledged. All comments and suggestions from the reviewers are sincerely appreciated. Our sincere thanks are due to Professor R. Ahlrichs (Karlsruhe, Germany) for his continued support of this work.

References

[1] T.F. Degnan Jr., C.M. Smith, C.R. Venkat, Appl. Catal. A 221 (2001) 283.
[2] G. Bellussi, G. Pazzuconi, C. Perego, G. Girouit, G. Terzonit, J. Catal. 157 (1995) 227.
[3] C.R.A. Catlow, Modeling of Structure and Reactivity in Zeolite, Academic Press, San Diego, CA, 1992.
[4] B. Kontnik-Matecka, M. Gorska, J. Eysymott, A. Salek, J. Mol. Struct. 80 (1982) 199.
[5] B.V. Liengme, W.K. Hall, Trans. Faraday Soc. 62 (1966) 3229.
[6] N.W. Cant, W.K. Hall, J. Catal. 25 (1972) 161.
[7] Y. Du, H. Wang, S. Chen, J. Mol. Catal. A 179 (2002) 253.
[8] J.L. White, L.W. Beck, J.F. Haw, J. Am. Chem. Soc. 114 (1992) 6182.
[9] E.G. Derouane, J.B. Nagy, J.P. Gilson, Z. Gabrlica, Stud. Surf. Sci. Catal. 7 (1981) 1412.
[10] E.N. Coker, C. Jia, H.G. Karge, Langmuir 16 (2000) 1205.
[11] R. Shah, J.D. Gale, M.C. Payne, Chem. Commun. (1997) 131.
[12] Y. Jeanvoine, J.G. Angyan, G. Kresse, J. Hafner, J. Phys. Chem. B 102 (1998) 5573.
[13] H.I. Hillier, J. Mol. Struct. (Theochem.) 463 (1999) 45.
[14] J. Limtrakul, S. Jungsuttiwong, P. Khongpracha, J. Mol. Struct. 525 (2000) 153.
[15] J. Sauer, M. Sierka, J. Comput. Chem. 21 (2000) 1470.

[16] J. Sauer, P. Ugliengo, E. Garrone, V.R. Saunders, Chem. Rev. 94 (1994) 2095.
[17] J. Sauer, Chem. Rev. 89 (1989) 199.
[18] J. Limtrakul, Chem. Phys. 193 (1995) 79.
[19] J. Limtrakul, P. Treesukol, C. Ebner, M. Probst, Chem. Phys. 215 (1997) 77.
[20] P.E. Sinclair, A.H. de Vries, P. Sherwood, C.R.A. Catlow, R.A. van Santen, J. Chem. Soc., Faraday Trans. 94 (1998) 3401.
[21] M. Brandle, J. Sauer, J. Am. Chem. Soc. 120 (1998) 1556.
[22] S.P. Greatbanks, I.H. Hillier, N.A. Burton, P. Sherwood, J. Chem. Phys. 105 (1996) 3370.
[23] R.Z. Khaliullin, A.T. Bell, V.B. Kazansky, J. Phys. Chem. A 105 (2001) 10454.
[24] J. Limtrakul, T. Nanok, P. Khongpracha, S. Jungsuttiwong, T.N. Truong, Chem. Phys. Lett. 349 (2001) 161.
[25] A.H. de Vries, P. Sherwood, S.J. Collins, A.M. Rigby, M. Rigutto, G.J. Kramer, J. Phys. Chem. B 103 (1999) 6133.
[26] M. Svensson, S. Humbel, R.D.J. Froese, T. Matsubara, S. Sieber, K. Morokuma, J. Phys. Chem. (1996) 19357.
[27] S. Dapprich, I. Komaromi, K.S. Byun, K. Morokuma, M.J. Frisch, J. Mol. Struct. (Theochem.) 461 (1999) 1.
[28] H.R. Tang, K.N. Fan, Chem. Phys. Lett. 330 (2000) 509.
[29] I. Roggero, B. Civalleri, P. Ugliengo, Chem. Phys. Lett. 341 (2001) 625.
[30] K. Sillar, P. Burk, J. Mol. Struct. (Theochem.) 589 (2002) 281.
[31] C. Raksakoon, J. Limtrakul, J. Mol. Struct. (Theochem.) 2003, in press.
[32] X. Solans-Monfort, J. Bertran, V. Branchadell, M. Sodupe, J. Phys. Chem. B 106 (2002) 10220.
[33] A. Damin, F. Bonino, G. Ricchiardi, S. Bordiga, A. Zecchina, C. Lamberti, J. Phys. Chem. B 106 (2002) 7524.
[34] M. Torrent, T. Vreven, D.G. Musaev, K. Morokuma, J. Am. Chem. Soc. 124 (2002) 192.
[35] P.B. Venuto, L.A. Hamilton, P.S. Landis, J. Catal. 5 (1966) 484.
[36] K.A. Becker, H.G. Karge, W.D. Streubel, J. Catal. 28 (1973) 403.
[37] A. Corma, V. Martinez-Soria, E. Schnoeveld, J. Catal. 192 (2000) 163.
[38] M. Sierka, J. Sauer, J. Phys. Chem. B 105 (2001) 1603.
[39] D.H. Olson, E. Dempsey, J. Catal. 13 (1969) 221.
[40] J.R. Hill, C.M. Freeman, B. Delley, J. Phys. Chem. A 103 (1999) 3772.
[41] A.K. Rappe, C.J. Casewit, K.S. Colwell, W.A. Goddard, W.M. Skiff, J. Am. Chem. Soc. 114 (1992) 10024.
[42] A. Pelmenschikov, J. Leszczynski, J. Phys. Chem. B 103 (1999) 6886.
[43] T.A. Wesolowski, O. Parisel, Y. Ellinger, J. Weber, J. Phys. Chem. A 101 (1997) 7818.
[44] E.G. Derouane, C.D. Chang, Micropor. Mesopor. Mater. 35–36 (2000) 425.
[45] L.A. Clark, M. Sierka, J. Sauer, J. Am. Chem. Soc. 125 (2003) 2136.
[46] A.M. Vos, X. Rozanska, R.A. Schoonheydt, R.A. van Santen, F. Hutschka, J. Hafner, J. Am. Chem. Soc. 123 (2001) 2799.
[47] X. Rozanska, R.A. van Santen, F. Hutschka, J. Hafner, J. Am. Chem. Soc. 123 (2001) 7655.
[48] M.J. Frisch, G.W. Trucks, H.B. Schlegel, G.E. Scuseria, M.A. Robb, J.R. Cheeseman, V.G. Zakrzewski, J.A. Montgomery, R.E. Stratmann Jr., J.C. Burant, S. Dapprich, J.M. Millam, A.D. Daniels, K.N. Kudin, M.C. Strain, O. Farkas, J. Tomasi, V. Barone, M. Cossi, R. Cammi, B. Mennucci, C. Pomelli, C. Adamo, S. Clifford, J. Ochterski, G.A. Petersson, P.Y. Ayala, Q. Cui, K. Morokuma, P. Salvador, J.J. Dannenberg, D.K. Malick, A.D. Rabuck, K. Raghavachari, J.B. Foresman, J. Cioslowski, J.V. Ortiz, A.G. Baboul, B.B. Stefanov, G. Liu, A. Liashenko, P. Piskorz, I. Komaromi, R. Gomperts, R.L. Martin, D.J. Fox, T. Keith, M.A. Al-Laham, C.Y. Peng, A. Nanayakkara, M. Challacombe, P.M.W. Gill, B. Johnson, W. Chen, M.W. Wong, J.L. Andres, C. Gonzalez, M. Head-Gordon, E.S. Replogle, J.A. Pople, Gaussian'98, Gaussian, Inc., Pittsburgh, PA, 2001.
[49] D. Frende, J. Klinowski, H. Hamdan, Chem. Phys. Lett. 149 (1988) 355.